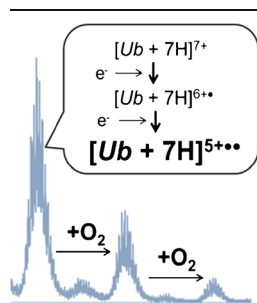**ASMS**

RESEARCH ARTICLE

Capturing Polyradical Protein Cations after an Electron Capture Event: Evidence for their Stable Distonic Structures in the Gas Phase

Takashi Baba, J. Larry Campbell

Sciex, 71 Four Valley Drive, Concord, ON L4K 4V8, Canada

Abstract. We report on the formation and "capture" of polyradical protein cations after an electron capture event. Performed in a unique electron-capture dissociation (ECD) instrument, these experiments can generate reduced forms of multiply protonated proteins by sequential charge reduction using electrons with ~1 eV. The true structures of these possible polyradicals is considered: Do the introduced unpaired electrons recombine quickly to form a new two-electron bond, or do these unpaired electrons exist as radical sites with appropriate chemical reactivity? Using an established chemical probe—radical quenching with molecular oxygen—we demonstrate that these charge-reduced protein cations are indeed polyradicals that form adducts with up to three molecules of oxygen (i.e., tri-radical protein cations) that are stable for at least 100 ms.

Keywords: Polyradical, Radical, Protein, Electron capture dissociation, Charge reduced species

Introduction

Electron capture dissociation (ECD) [1, 2] and electron transfer dissociation (ETD) [3] are two widely used dissociation techniques in mass spectrometry. Their popularities, particularly in the realm of proteomics, stem from their abilities to provide complete sequence coverage across entire polypeptide backbones [1, 2], top down protein sequencing [4], and de novo sequencing [5, 6]. ECD and ETD also retain fragile post-translational modifications, including glycosylation [7, 8], at their sites of bonding. The fragmentation mechanism for ECD and ETD involve radical driven dissociations, with an unpaired electron provided to a multiply protonated peptide/protein by either an electron beam (ECD) [1, 2] or by electron transfer from reagent anions (ETD) [3].

However, it is quite common for both ECD and ETD to yield abundant amounts of charge-reduced but undissociated protein cations [1–3]. These products, often termed charge-reduced species (CRS) or electron capture no dissociation (EC no D) species,

have an odd number of electrons and are radical in nature. When additional energy is added to these ions by collisions with a target gas or by IR laser activation, typical ECD/ETD fragments, c' and z• ions, are produced [9–11]. This suggests that these CRS are long-lived radical cation intermediates that have formed a stable structure. In fact, protein cations can capture multiple electrons in ECD/ETD as a consequence of sequential electron capture/transfer events [1–3]. These are reactions for multiple charge-reduced species, CR^nS, where n = the number of charges reduced in the intact species. Interestingly, the reduced charges for these protonated proteins do not decrease the mass of the system, as the once charged protons are still present as hydrogen.

A curious question about CR^nS is whether or not they behave chemically as a radical. Kleinnijenhuis and coworkers [12] raised such a question in their study of doubly charge reduced lantibiotic peptides. They postulated that either "…the induced radical sites could recombine to form a new two-electron pair, or they will not recombine and two fixed or mobile radical sites will remain present in the ion." Based upon collision-induced dissociation of the triply protonated lanticin peptide and a CR^2S form, they concluded that the radicals had recombined to form a new bond. However, the fact that some $[M + 4H]^{2+}$ ions are able to fragment to lose H• radical points to the existence of two separated radical sites. However, the lanticin peptide, bearing three intramolecular disulfide

Correspondence to: Takashi Baba; e-mail: takashi.baba@sciex.com

bonds—which are known to be structural foci of electron capture/transfer events [13] —could itself be a special case where multiple radical sites are generated in close proximity because of existing structural constraints.

Besides observing how potential polyradical protein/peptide cations fragment, chemical probes can also be used to detect radical sites in CRS. For example, Xia and coworkers reported that ETD-generated z• fragment ions—with an unpaired electron on α-carbon—reacted with O_2 to form adducts [14]. In addition to z ions, the CRS formed from ETD also reacted analogously with O_2. Their experiments, conduced with an rf ion trap, demonstrated the device's applicability for such diagnostic ion-molecule reactions [15] because the ions are confined in the relatively high pressure (~0.1 Pa) of neutral gas. In addition, their use of molecular oxygen served to probe for "distonic" radical cations [16, 17] (i.e., the site of positive charge and the radical site are physically separated in the ion's structure), as this ion/molecule reaction had been used for this purpose previously [18, 19]. In our present study, we have examined the radical reactivity of several protein cations after charge reduction in a novel ECD instrument [20]. Upon reaction with O_2, several protein cations formed multiple adducts that essentially have recombined all of the free radical sites present on the CRS.

Experimental

All peptides and proteins used in this research were purchased from Sigma Aldrich (Oakville, ON, Canada). Peptides used in this study were bee melittin (26 amino acids - aa), human β-endorphin (31 aa), and gila monster exenatide (36 aa). Proteins used in this study were bovine ubiquitin (Ub) (76 aa), equine cytochrome c (CYCS) (104 aa), equine myoglobin (MB) (153 aa), and bovine carbonic anhydrase 2 (CA2) (259 aa). The samples were dissolved in water:acetonitrile:formic acid (49.9:50.0:0.1) to concentrations of 5 μM each. Each solution was infused individually with flow rate of 3.3 μL/min and ionized by electrospray ionization (ESI) using a DuoSpray® ion source (Sciex). ESI voltage was +5500 V.

Details of the electron-ion reaction device (ECD cell) (Figure 1) and the mass spectrometer used in this research were described previously [20], with the addition of N52 grade neodymium magnets (K & J Magnetics Inc. Pipersville, PA, USA) to replace the weaker N42 grade magnets. The 14% increase of magnetic flux density improved electron capture efficiency by about a factor of three (data not shown). He buffer
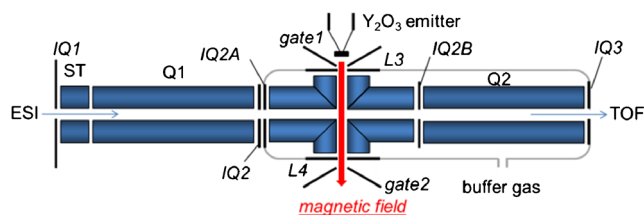

Figure 1. ECD devices using a blanched rf ion trap placed between Q1 and Q2

gas (99.999%) was introduced into Q2 and the ECD cell through a pipe on the Q2 housing, and the partial pressure of He was calculated as 1.3 Pa using pumping speed, monitoring pressure, and conductance of orifices on IQ2A and IQ3 calibrated for He. Air could also be introduced into the same He gas pipe through a leak valve when additional oxygen was required to enhance $+O_2$ reaction product ions. For some experiments, residual oxygen in vacuum was used for $+O_2$ reaction. The base pressure in the chamber that stored the ST, Q1, ECD cell, and Q2 was 3.7×10^{-4} Pa.

A conventional trapping mode was used for these ECD reactions instead of the previously reported simultaneous trapping mode [20]. Precursor ions isolated by Q1 were introduced into the ECD cell, and then trapped by raising the voltage of the IQ2A lens. For ECD, electrons were irradiated for 5–20 ms by opening gate 1, after which time the electron beam was stopped by closing gate 2. These ECD reaction times were chosen to maximize the signal of any CR^nS species ($n \geq 2$) for the multiply protonated proteins. The stored ions were kept in the ECD cell for 50–100 ms to allow $+O_2$ reaction before extracting all ions to the TOF mass spectrometer through Q2. The TOF mass spectrometer acquired spectra continuously with total data accumulation times from 500 to 1000 s. The $+O_2$ reaction was applied to the ECD products by the same ECD conditions but with air introduced through the leak valve. Partial pressure of oxygen in the ECD cell was 13 mPa. CRS and CR^2S mass spectra were recorded by signal accumulation for 1000 s. While the resolving power of our TOF mass spectrometer was not good enough to separate isotopic peak profile in case of cytochrome C (CYCS), myoglobin (MB) and carbonic anhydrase 2 (CA2), the recorded isotopic envelopes were compared with theoretical m/z values for the detected $+O_2$ species.

Results and Discussion

In our present study, we first probed the CRS forms of protonated ubiquitin ($[Ub + 7H]^{7+}$) for radical reactivity with O_2 (Figure 2). After isolating the isotopic envelope of $[Ub + 7H]^{7+}$ (red), these ions were subjected to ECD (0.5 eV electron kinetic energy) and their CRS products detected without O_2 present (Figure 2b and c). Comparing the mass spectra of the $[Ub + 6H]^{6+}$ (red) and the CRS form derived from reduction of $[Ub + 7H]^{7+}$ ions (blue), we can observe the ~1/6 m/z unit shift corresponding to the additional hydrogen radical – $[Ub + 7H]^{6+\bullet}$ versus the lighter $[Ub + 6H]^{6+}$ (Figure 2b). An analogous shift is observed for $[Ub + 7H]^{5+\bullet\bullet}$ (Figure 2c).

We then introduced O_2 into the ECD cell to probe the CRS population for radical cations. Interestingly, we observed $+O_2$ reactions for only the CRS species in our experiments; no closed-shell even-electron protein cations formed $+O_2$ adducts. For example, there were no $[Ub + 7H + O_2]^{7+}$ product ions (Figure 1a), which would have resulted from the addition of O_2 to the Q1-isolated precursor protein ions unaffected by the ECD process (i.e., they have not captured an electron as
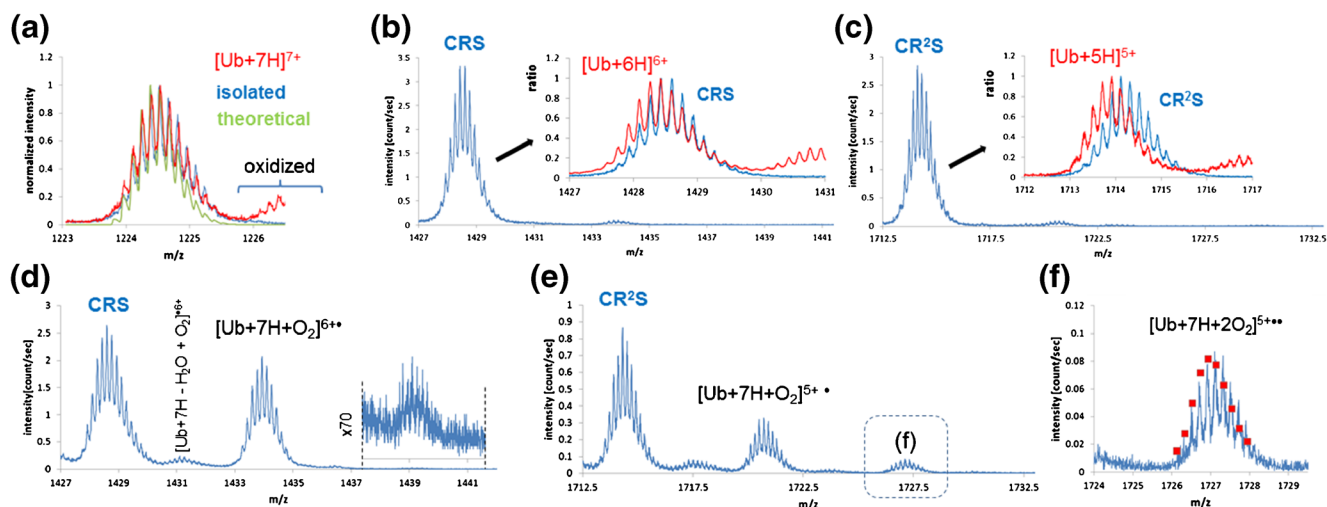
Figure 2. **(a)** Mass spectrum of $[Ub + 7H]^{7+}$ before isolation by quadrupole filter: Q1 (red trace), after isolation (blue), and the theoretical isotopic distribution (green). **(b)** After ECD of $[Ub + 7H]^{7+}$, CRS products corresponding to $[Ub + 7H]^{6+\bullet}$ were generated (blue) that are ~1/6 m/z unit heavier than the $[Ub + 6H]^{6+}$ analogue (red). **(c)** During the same ECD event as **(b)**, CR^2S products corresponding to $[Ub + 7H]^{5+\bullet\bullet}$ were generated (blue) that are ~2/5 m/z unit heavier than the $[Ub + 5H]^{5+}$ analogue (red). **(d)** Upon addition of O_2 to the cell, $[Ub + 7H + O_2]^{6+\bullet}$ formed, indicating the existence of a radical; $[Ub + 6H + 2O_2]^{6+\bullet\bullet}$ is also observed to form via an unknown mechanism. **(e)** During the same ion/molecule reaction as **(d)**, the CR^2S product forms not one, but two adducts with O_2: $[Ub + 7H + O_2]^{5+\bullet\bullet}$ and $[Ub + 7H + 2O_2]^{5+\bullet\bullet}$. **(f)** Inset from **(e)** showing formation of $[Ub + 7H + 2O_2]^{5+\bullet\bullet}$, indicating the existence of a biradical (red squares show theoretical isotopic distribution for $[Ub + 7H + 2O_2]^{5+\bullet\bullet}$).

evidenced by their static charge state). Although the gas-phase oxidation of methionine side chains might be possible, it did not occur during the time scale of our ECD experiments and was not a factor. For the first CRS of $[Ub + 7H]^{7+}$, an intense signal for the $[Ub + 7H + O_2]^{6+\bullet}$ product ion was observed, revealing itself as a monoradical [6, 14, 18, 19]. Addition of O_2 to another CRS, $[Ub + 7H – H_2O + O_2]^{6+\bullet}$ was also recorded in the mass spectrum. Also of note was the detection of a very weak $+2O_2$ product (0.3% compared with the CRS) equivalent to $[Ub + 6H + 2O_2]^{6+\bullet\bullet}$. This type of unexpected reaction product was also observed during the analysis of exenatide, and may arise as a consequence of the formation of a peroxyl radical after addition of molecular oxygen to the monoradical cation. This peroxyl radical can itself engage in another radical reaction via an intramolecular hydrogen transfer; such scenarios have been postulated to play roles in oxidative protein damage [21–25] and during hydrocarbon combustion processes [26, 27]. In our ECD experiments, the newly formed peroxyl radical could abstract a hydrogen atom, likely from an amino acid side chain close to the $+O_2$ reaction site, as has been postulated by Moore and coworkers [28]. Arguably, the use of a distonic radical reagent like dimethyl disulfide [29, 30] would have avoided the potential for such radical reaction cascading upon the formation of a radical-quenching thiomethyl adduct. However, given that the intensities of the ubiquitin- and the melittin-based examples of this "double oxygen addition to a monoradical" are among the smallest in our data sets, we can infer that this intramolecular hydrogen atom transfer process is rare. In contrast, we observe much more intense signals (i.e., ~10× higher than the aforementioned "monoradical $+2O_2$" species) for product ions resulting from

the formation of double oxygen adducts with other charge reduced species (i.e., ≥2 electrons captured). For example, in Figure 2e, we observe a significant population of ions at m/z 1726.13 (monoisotopic m/z), which is consistent with formation of $[M + 7H + 2O_2]^{5+}$. This two O_2 attachment is direct evidence that the CR^2S from the ubiquitin precursor (Z = 7+) is a biradical.

Based upon these results, we postulate that the CR^2S population is a mixture of at least four different structures: (1) where there are two separated unpaired electrons on the polypeptide backbone, (2) a structure where the unpaired electrons have recombined, (3) two unpaired electrons are on basic groups (i.e., no $+O_2$ reactivity), (4) one of the unpaired electrons is on a basic group groups (i.e., no $+O_2$ reactivity) and another is on the polypeptide backbone groups (i.e., exhibits $+O_2$ reactivity). In addition, the lifetimes of the biradical states were at least ~100 ms because the $+O_2$ reaction was continuously observed for 100 ms after the ECD reaction. As shown in Figure ESM-1(electronic supplementary material), $+O_2$ and $+2O_2$ reactivity were not affected by electron kinetic energy (KE) for ECD. This means that the radical sites are stable once they are generated.

To confirm the existence of biradicals, we examined the reaction kinetics for the reaction of O_2 with the CRS and CR^2S forms of Ub. Figure 3a shows an observed $+O_2$ progress on the CRS group. Sixty-one percent of produced CRS were reacted with O_2, but others were not. Although CRS is an odd electron species (Figure 2b), it displays two different $+O_2$ reactivities, implying that this CRS population contains at least two types of radical structures. We postulate that 61% of CRS has its unpaired electron on a backbone α-carbon that reacts with O_2
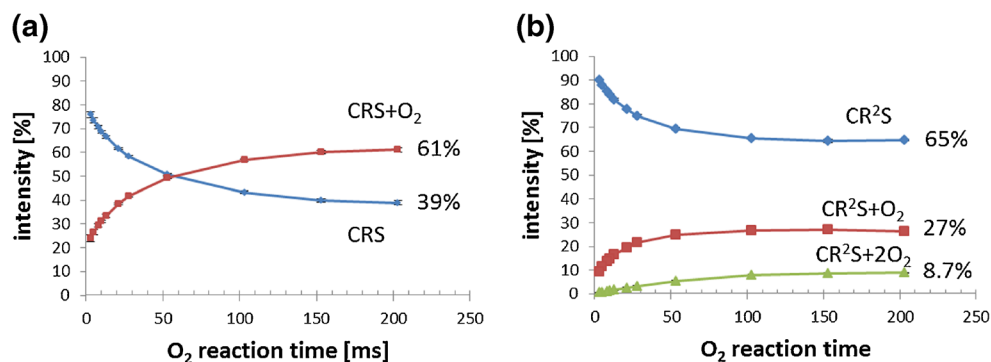
Figure 3. Temporal profiles for the reaction of the CRS **(a)** and (CR^{2}S) **(b)** forms of [Ub + 7H]$^{7+}$ with O$_2$

readily [31]. The remaining 40% of the CRS population has an apparently lower rate of reaction with O$_2$. This may be the result of several possible factors: the radical is located on a residue that is sterically hindered to O$_2$; the radical site is less reactive given its position/location (i.e., a nitrogen-centered radical). [Minor ECD products: c•, whose dissociation termini is nitrogen do not show +O$_2$ reactivity.]

Similar patterns in reactivity were observed with the Ub reduced by two electron capture events (CR^{2}S). After ~150 ms of reaction time, the +O$_2$ reaction with the CR^{2}S ions plateaued, similar to the CRS reaction. Only 27% of the CR^{2}S population reacted to form a single adduct with O$_2$, while 8.8% of CR2S reacted with two O$_2$. The high amount of unreacted CR^{2}S ions was unexpected if one assumes that the two radical sites behave as independent entities; if each radical on the CR^{2}S reacted to the same extent as the CRS monoradical, we would have predicted that 84% of the CR^{2}S population [100% – (40% × 40%) = 84%] should have formed adducts with either one or two O$_2$ molecules. However, only 36% [27% (+O$_2$) + 9% (+2O$_2$)] reacted, falling well short of this mark. Alongside the possible reasons for unreactive CRS ions, the CR^{2}S species could undergo radical–radical recombination to form a new chemical bond, thereby losing the ion's radical reactivity [12]. In case of melittin, this recombination rate is 100% and no radical reactivity is observed (i.e., no +O$_2$ reactions detected) (Figure ESM-2). Similar to the CRS monoradical, the CR^{2}S + O$_2$ product ion (27%) remains a biradical, albeit one where one radical is a newly formed alkoxy radical (i.e., at the site of O$_2$ addition), whereas the

second radical may be located at a basic group in Arg, Lys, His, or the N terminus with no +O$_2$ reactivity.

In addition to CR^{2}S, CR^{3}S, and CR^{4}S product ions were observed for other proteins, including melittin (Figure ESM-2), along with their +O$_2$ adducts. The intensity ratio to the oxygen adducts compared with the total nth charge-reduced signal (CR^{n}S + [CR^{n}S + O$_2$] + [CR^{n}S + 2O$_2$]) are displayed in Figure 4. These ratios, determined from their ECD spectra (Figure ESM-2), depict the CR^{n}S and +O$_2$ products and some interesting features. For example, the single +O$_2$ species for CR^{2}S has a 0% value (Figure 4a) because the observed +O$_2$ adduct formed from the monoradical [M + 3H]$^{2+•}$ (i.e., CR^{2}S that lost one H•, a well-known by-product of ECD [Figure 4a]) instead of the intact biradical [M + 4H]$^{2+••}$. Conversely, the CR^{n}S product ions of [Ub + 7H]$^+$ were somewhat more stable, producing +nO$_2$ products (Figure 4b). (N.B. Ratios were lower than Figure 3a due to a shorter reaction time used to collect the data—25 ms versus >100 ms). For melittin (Figure 4a), the single unpaired electron was stable in CRS, but no +O$_2$ adduct was observed for CR^{2}S for several possible reasons as outlined for the case of [Ub+7H]$^{7+}$ (vide supra). However, an +O$_2$ adduct did form with the CR^{3}S ion upon the introduction of the third and unpaired reactive radical, which was stable, unlike the unreactive/recombined first pair of radicals.

Based upon the observed reactivity of the CR^{2}S form of several protein ions (Figure 5), we postulate that the average distance between radical sites played a key role in the variability observed between proteins. For example, radical reactivity was greater for ubiquitin than for melittin (e.g., more +2O$_2$
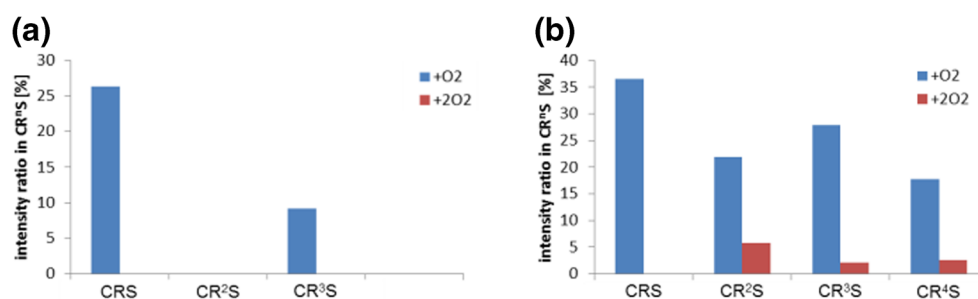

Figure 4. +O$_2$ and +2O$_2$ reactivity of multiply charge reduced ions. **(a)** [M + 4H]$^{4+}$ of melittin, and **(b)** [M + 7H]$^{7+}$ of Ub
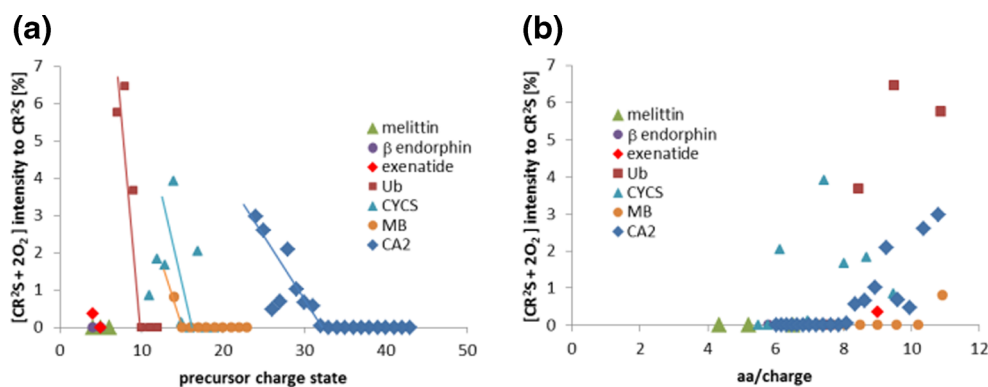
Figure 5. Intensity ratio of +2O$_2$ adducts to the CR^{2}S product as a function of **(a)** precursor charge states and **(b)** the normalized number of amino acids (aa) per charge residue of the precursor

adduct formation for the CR^{n}S of Ub), suggesting lower degrees of radical recombination that would shut down the +2O$_2$ reaction channel. However, for Ub we also observed decreasing relative amounts of +2O$_2$ adducts with higher degrees of CR^{n}S; again, radical recombination between the newly formed unpaired electron and another radical on the CRS would compete with +2O$_2$ adduct formation. Figure 5 displays the relationships between the observed radical reactivity of several protein as a function of (Figure 5a) precursor charge states and (Figure 5b) lengths of amino acid chain per charge. Formation of +2O$_2$ adducts were observed for proteins larger than ubiquitin, but not for smaller proteins (e.g., melittin, β-endorphin, exenatide). On average, when protons were separated on the proteins by ~6–8 aa, +2O$_2$ adducts were observed (Figure 5b). This "distance" results in a ~0.5 eV repulsive Coulomb potential between adjacent charges (assuming an approximate separation of ~0.4 nm between protein backbone α-carbons). For proteins bearing two added protons separated by less than ~6 aa, higher degrees of ECD efficiencies (i.e., more complete dissociation and less intense signals for CR^{n}S) were observed. This results mainly from a higher repulsive Coulomb potential among these charges and more efficient protein amide backbone fragmentation. When CR^{2}S products cooled collisionally within the ECD cell to a sufficient degree, these polyradical species were stabilized such that they could

react with oxygen instead of dissociating. However, the higher charge states of each protein yielded fewer +2O$_2$ adducts for the CR^{2}S products. One possible reason for this observation is that the radicals that have migrated to the α-carbon position along the protein backbone (i.e., the +O$_2$ reactive species) rapidly dissociate to c and z• ions in part attributable to the higher degree of Coulombic repulsion (<8 aa/charge, Figure 5b and Figure ESM-3). The CRS and CR^{2}S products that bear radical sites along the side chains of the protein should not dissociate as readily, nor should they engage in as rapid an +O$_2$ adduct formation as the α -carbon radical analogues.

We also probed for the presence of CR^{n}S products bearing more than three independent radical sites. During the ECD of [Ub + 7H]$^{7+}$, a small number of triradicals and tetraradicals were identified in the form of +3O$_2$ adducts (Figure 6). Similar to the CR^{2}S product, we postulate that radical recombination served to decrease the observed radical reactivity for the CR^{4}S product. However, the amount of +2O$_2$ adducts increased slightly compared with the CR^{3}S product (2.1% to 2.6%, Figure 4b) because of the additional unpaired electrons. These mixtures of recombined and isolated radicals suggest that these radical sites survive when they are spatially separated from each other. Although these +3O$_2$ adducts, observed for both CR^{3}S (Figure 6a) and CR^{4}S (Figure 6b) exhibited very low intensities (<0.4%) relative to the CRS product, their
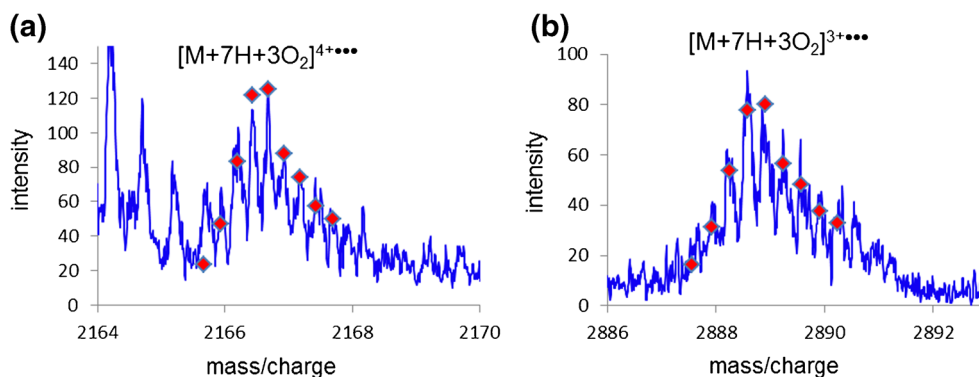

Figure 6. Possible evidence for triradicals in the form of CR^{n}S + 3O$_2$ from ECD of [Ub + 7H]$^{7+}$. Expanded profiles of possible triradical product: **(a)** CR^{3}S + 3O$_2$, and **(b)** CR^{4}S + 3O$_2$. Full spectrum is shown in Supplementary Figure ESM-4

isotopic profiles matched the theoretical distribution for the predicted adducts. No additional oxygen adducts were observed. Based upon our aforementioned estimates, we estimate a minimum distance for separation of radical sites at between ~25–40 aa (~10–16 nm) to avoid facile recombination. This estimate is based upon ubiquitin's 76 aa length and the fact that triradicals were observed as $+3O_2$ adducts but tetraradicals were not observed as $+4O_2$ adducts. Since the gas-phase forms of protonated Ub is known to retain three-dimensional conformations [32], specifically the $[Ub + 7H]^{7+}$ form we examined here, we cannot discount that radical sites will be closer than our approximations. Conformations may also serve to hinder radical recombination, but the nature of conformation effect on biradical stability is not clear at this time.

Conclusion

We have confirmed the formation of stable biradical and even triradical species after electron capture of protonated proteins. By monitoring formation of $+O_2$ adducts, we confirmed the presence of distonic radicals (charge-radical separation) within many proteins. These polyradicals can survive for extended periods of time in the mass spectrometer's environment when individual radicals are separated by ~20–40 amino acid residues.

Acknowledgments

References

1. Zubarev, R.A., Kelleher, N.L., McLafferty, F.W.: Electron capture dissociation of multiply charged protein cations. A nonergodic process. J. Am. Chem. Soc. **120**, 3265–3266 (1998)
2. Zubarev, R.A., Horn, D.M., Fridriksson, E.K., Kelleher, N.L., Kruger, N.A., Lewis, M.A., Carpenter, B.K., McLafferty, F.W.: Electron capture dissociation for structural characterization of multiply charged protein cations. Anal. Chem. **72**, 563–573 (2000)
3. Syka, J.E.P., Coon, J.J., Schroeder, M.J., Shabanowitz, J., Hunt, D.F.: Peptide and protein sequence analysis by electron transfer dissociation mass spectrometry. PNAS **101**, 9528–9533 (2004)
4. Ge, Y., Lawhorn, B.G., El-Naggar, M., Strauss, E., Park, J.-H., Begley, T.P., McLafferty, F.W.: Top down characterization of larger proteins (45 kDa) by electron capture dissociation mass spectrometry. J. Am. Chem. Soc. **124**, 672–678 (2002)
5. Horn, D.H., Zubarev, R.A., McLafferty, F.W.: Automated de novo sequencing of proteins by tandem high-resolution mass spectrometry. PNAS **97**, 10313–10317 (2000)
6. Baba, T., Greene, T., Glish, G.L.: Electron Capture Dissociation de novo sequencing by C- and Z- terminal fragment discrimination using neutral-radical reaction. The 57th Annual Meeting of the American Society for Mass Spectrometry Conference on Mass Spectrometry and Allied Topics, Philadelphia, PA (2009)
7. Mirgorodskaya, E., Roepstorff, P., Zubarev, R.A.: Localization of O-glycosylation sites in peptides by electron capture dissociation in a Fourier transform mass spectrometer. Anal. Chem. **71**, 4431–4436 (1999)
8. Manri, N., Satake, H., Kaneko, A., Hirabayashi, A., Baba, T., Sakamoto, T.: Glycopeptide identification using liquid-chromatography-compatible hot electron capture dissociation in a radio-frequency-quadrupole ion trap. Anal. Chem. **85**, 2056–2063 (2013)
9. Horn, D.M., Ge, Y., McLafferty, F.W.: Activated ion electron capture dissociation for mass spectral sequencing of larger (42 kDa) Proteins. Anal. Chem. **72**, 4778–4784 (2000)
10. Lin, C., Cournoyer, J.J., O'Connor, P.B.: Probing the gas-phase folding kinetics of peptide ions by IR Activated DR-ECD. J. Am. Soc. Mass Spectrom. **19**, 780–789 (2008)
11. Ledvina, A.R., McAlister, G.C., Gardner, M.W., Smith, S.I., Madsen, J.A., Schwartz, J.C., Stafford Jr., G.C., Syka, J.E.P., Brodbelt, J.S., Coon, J.J.: Infrared photoactivation reduces peptide folding and hydrogen-atom migration following ETD tandem mass spectrometry. Angew. Chem. **121**, 8678–8680 (2009)
12. Kleinnijenhuis, A.J., Heck, A.J.R., Duursma, M.C., Heeren, R.M.A.: Does double electron capture lead to the formation of biradicals? An ECD-SORI-CID study on lacticin 481. J. Am. Soc. Mass Spectrom. **16**, 1595–1601 (2005)
13. Zubarev, R.A., Kruger, N.A., Fridriksson, E.K., Lewis, M.A., Horn, D.M., Carpenter, B.K., McLafferty, F.W.: Electron capture dissociation of gaseous multiply-charged proteins is favored at disulfide bonds and other sites of high hydrogen atom affinity. J. Am. Chem. Soc. **121**, 2857–2862 (1999)
14. Xia, Y., Chrisman, P.A., Pitteri, S.J., Erickson, D.E., McLuckey, S.A.: Ion/molecule reactions of cation radicals formed from protonated polypeptides via gas-phase ion/ion electron transfer. J. Am. Chem. Soc. **128**, 11792–11798 (2006)
15. Dehmelt, H.G.: Radiofrequency spectroscopy of stored ions II: spectroscopy. Adv. At. Mol. Phys. **5**, 109–154 (1969)
16. Yates, B.F., Bouma, W.J., Radom, L.: Detection of the prototype phosphonium (CH_2PH_3), sulfonium (CH_2SH_2), and chloronium (CH2ClH) ylides by neutralization-reionization mass spectrometry: a theoretical prediction. J. Am. Chem. Soc. **106**, 5805–5808 (1984)
17. Yates, B.F., Bouma, W.J., Radom, L.: Distonic radical cations: guidelines for the assessment of their stability. Tetrahedron **42**, 6225–6234 (1986)
18. Yu, S.J., Holliman, C.L., Rempel, D.L., Gross, M.L.: The.beta.-distonic ion from the reaction of pyridine radical cation and ethene: a demonstration of high-pressure trapping in Fourier transform mass spectrometry. J. Am. Chem. Soc. **115**, 9676–9682 (1993)
19. Kirk, B.B., Harman, D.G., Blanksby, S.J.: Direct observation of the gas phase reaction of the cyclohexyl radical with dioxygen using a distonic radical ion approach. J. Phys. Chem. A **114**, 1446–1456 (2010)
20. Baba, T., Campbell, J.L., Le Blanc, J.C.Y., Hager, J.W., Thomson, B.A.: Electron capture dissociation in a branched radio-frequency ion trap. Anal. Chem. **87**, 785–792 (2015)
21. Davies, K.J.A.: Protein damage and degradation by oxygen radicals. I. General aspects. J. Biol. Chem. **262**, 9895–9901 (1987)
22. Davies, K.J.A., Delsignore, M.E., Lin, S.W.: Protein damage and degradation by oxygen radicals. II. Modification of amino acids. J. Biol. Chem. **262**, 9902–9907 (1987)
23. Davies, K.J.A., Delsignore, M.E.: Protein damage and degradation by oxygen radicals. III. Modification of secondary and tertiary structure. J. Biol. Chem. **262**, 9908–9913 (1987)
24. Davies, K.J.A., Delsignore, M.E., Pacifici, R.E.: Protein damage and degradation by oxygen radicals. IV. Degradation of denatured protein. J. Biol. Chem. **262**, 9914–9920 (1987)
25. Hawkins, C.L., Davies, M.J.: Generation and propagation of radical reactions on proteins. Biochim. Biophys. Acta **1504**, 196–219 (2001)
26. Sheng, C.Y., Bozzelli, J.W., Dean, A.M., Chang, A.Y.J.: Detailed kinetics and thermochemistry of C_2H_5 + O_2: reaction kinetics of the chemically-activated and stabilized $CH_3CH_2OO•$ adduct. J. Phys. Chem. A **106**, 7276–7293 (2002)
27. Zhu, L., Bozzelli, J.W., Kardos, L.M.: Thermochemical properties, $\Delta fH°(298)$, $S°(298)$, and $Cp°(T)$, for n-Butyl and n-pentyl hydroperoxides and the alkyl and peroxy radicals, transition states, and kinetics for intramolecular hydrogen shift reactions of the peroxy radicals. J. Phys. Chem. A **111**, 6361–6377 (2007)
28. Moore, B.N., Blanksby, S.J., Julian, R.R.: Ion-molecule reactions reveal facile radical migration in peptides. Chem. Commun. 5015–5017 (2009)

29. Stirk, L.M., Orlowski, J.C., Leeck, D.T., Kenttämaa, H.I.: The identification of distonic radical cations on the basis of a reaction with dimethyl disulfide. J. Am. Chem. Soc. **114**, 8404–8406 (1992)

30. Stirk, L.M., Kiminkinen, L.K.M., Kenttämaa, H.I.: Ion-molecule reactions of distonic radical cations. Chem. Rev. **92**, 1649–1665 (1992)

31. Davies, M.J.: The oxidative environment and protein damage. Biochim. Biophys. Acta **1703**, 93–109 (2005)

32. Breuker, K., Oh, H., Lin, C., Carpenter, B.K., McLafferty, F.W.: Nonergodic and conformational control of the electron capture dissociation of protein cations. Proc. Natl. Acad. Sci. U. S. A. **101**, 14011–14016 (2004)